Acute slow wave responses to high-frequency gastric electrical stimulation in patients with gastroparesis defined by high-resolution mapping

Journal:

Neuromodulation

Running Title:

Mapping gastric electrical stimulation

Authors:

Timothy R. Angeli[1], Peng Du[1], David Midgley[1], Niranchan Paskaranandavadivel[1], Shameer Sathar[1], Christopher Lahr[2], Thomas L. Abell[3], Leo K. Cheng[1,4], Gregory O'Grady[1,5]

Affiliations:

[1]Auckland Bioengineering Institute, University of Auckland, Auckland, New Zealand.

[2]Department of Surgery, Mississippi Medical Center, Jackson, MS, USA.

[3]Department of Gastroenterology, University of Louisville, Louisville, KY, USA.

[4]Department of Surgery, Vanderbilt University, Nashville, TN, USA.

[5]Department of Surgery, University of Auckland, Auckland, New Zealand.

Financial Support:

This work was supported by the New Zealand Health Research Council, the National Institutes of Health (R01 DK64775), and the Medical Technologies Centre of

Research Excellence New Zealand. PD was supported by a Marsden Grant administered by the Royal Society of New Zealand. LKC was supported by a Fraunhofer-Bessel Research Award from the Alexander von Humboldt Foundation and the Fraunhofer IPA.

Authorship Statement:

Study concept and design: TRA, PD, TLA, LKC, GOG. Acquisition of data: TRA, PD, CL, TLA, LKC, GOG. Analysis and interpretation of data: TRA, PD, DM, NP, SS, TLA, LKC, GOG. Drafting of manuscript: TRA, GOG. The manuscript was critically reviewed and approved by all authors.

Conflicts of Interest Statement:

No authors have any direct financial interests in relation to the material presented in this paper. TRA, PD, NP, LKC, and GOG hold intellectual property and/or patent applications in the field of mapping gastrointestinal electrophysiology. TLA is a former licensor, consultant, and investigator for Medtronic, Inc.

Correspondence:

Dr. Gregory O'Grady

Department of Surgery, University of Auckland

Private Bag 92019, Auckland, New Zealand

+64 (0)27 422 2989; greg.ogrady@auckland.ac.nz

Abstract

Background and Aims

High-frequency gastric electrical stimulation (GES) has emerged as a therapy for gastroparesis, but the mechanism(s) of action remain unclear. There is a need to refine stimulation protocols for clinical benefit, but a lack of accurate techniques for assessing mechanisms in clinical trials, such as slow wave modulation, has hindered progress. We thereby aimed to assess acute slow wave responses to GES in gastroparesis patients using high-resolution (multi-electrode) mapping, across a range of stimulation doses achievable by the Enterra stimulation device (Medtronic Inc, MN).

Materials and Methods

Patients with medically-refractory gastroparesis (n=8) undergoing device implantation underwent intraoperative HR mapping (256 electrodes). Baseline recordings were followed by four protocols of increasing stimulation intensity, with washout periods. Slow wave patterns, frequency, velocity, amplitude, and dysrhythmia rates were quantified by investigators blinded to stimulation settings.

Results

There was no difference in slow wave pattern, frequency, velocity, or amplitude between baseline, washout, and stimulation periods (all $P>0.5$). Dysrhythmias included ectopic pacemakers, conduction blocks, retrograde propagation, and colliding wavefronts, and dysrhythmia rate were unchanged with stimulation off versus on (31% vs 36% duration dysrhythmic; $P>0.5$). Symptom scores and gastric emptying were improved at 5.8 month follow-up ($P<0.05$).

Conclusions

High-frequency GES protocols achievable from a current commercial device did not acutely modulate slow wave activity or dysrhythmias. This study advances clinical methods for identifying and assessing therapeutic GES parameters, and can be applied in future studies on higher-energy protocols and devices.

Key words:

High-resolution mapping; Electrophysiology; Diabetes mellitus; Pacing; Slow wave;

Abbreviations:

GES – gastric electrical stimulation

HR – high-resolution

ICC – interstitial cells of Cajal

cpm – cycles per minute

SD – standard deviation

SEM – standard error of the mean

FDA – Food and drug administration (USA)

FPC – flexible printed circuit

AT – activation time

GEMS – Gastrointestinal electrical mapping suite

Introduction

The management of gastroparesis remains challenging, with few effective therapies providing long-term proven benefit [1]. Patients with severe medically-refractory disease pose a particularly difficult clinical challenge, and often require intensive use of hospital resources [2,3].

In recent years, gastric electrical stimulation (GES) using high-frequency protocols has emerged as a therapeutic option in medically-refractory gastroparesis [4,5]. GES provides a regular injection of current into the gastric muscular layers, without entraining (pacing) gastric slow waves when used at current clinical doses [5,6]. A device is commercially available (Enterra, Medtronic, MN), having Humanitarian Device Exemption status from the FDA. Several reports in patients with medically-refractory gastroparesis have demonstrated marked symptom improvement using this device, as well as decreased reliance on invasive nutritional support [7]. Supporting evidence for the efficacy of high-frequency GES also comes from canine studies showing reduced emesis following therapy [8,9]. However, the clinical indications remain controversial, because most human studies have used open-label non-controlled designs [7].

Mechanisms of action for high-frequency GES have been investigated, including modification of central perceptions of nausea, modulation of vagal afferent pathways, and possible effects on slow waves [10–13]. However, a lack of accurate tools for assessing mechanisms such as slow wave modulation in clinical trials has prevented progress toward refining and improving stimulation approaches. For example, there

have been few clinical electrophysiology studies in gastroparesis patients [13], and none that have reliably mapped the effects on gastric dysrhythmia.

High-resolution (HR) electrical mapping is an emerging motility research strategy with potential to further inform stimulation mechanisms and responses [14]. HR mapping employs dense arrays of electrodes to define slow wave activation sequences in accurate spatiotemporal detail [15,16], and has recently been utilized to discover a range of complex spatial dysrhythmias underlying functional gastrointestinal disorders [17–19].

The present study applied HR mapping to investigate the electrophysiological effects of high-frequency GES protocols. *In-vivo* experimental studies were performed intraoperatively in patients with medically-refractory gastroparesis. Standard Enterra therapy protocols were evaluated [4,20], as well as a range of experimental protocols of higher stimulation intensity achievable within the dose-delivery capacity of the device.

Materials and Methods

Patient Population

Ethical approval for this work was granted by the Institutional Review Board of the University of Mississippi Medical Center. Consecutive patients undergoing implantation with GES devices (Enterra, Medtronic, MN) were recruited and gave informed consent. All patients had been diagnosed with medically-refractory gastroparesis, confirmed by standardized scintigraphy testing (≥10% gastric retention of standard meal at 4 hours) [21], and were free of malignancy, primary eating

disorders, or pregnancy. Demographic data, comorbidities, medical histories, and body mass index were recorded for each patient.

Symptom severity was assessed at baseline and post-implant as a total symptom score (TSS) for each patient. TSS was calculated by scoring five symptoms (pain, bloating / distension, nausea, vomiting, and early satiety) on a five-point Likert scale (0-absent, to 4-severe), which were then summed to yield the TSS, effectively an overall symptom severity metric out of a possible 20 points (0-absent, to 20-severe across all categories) [17].

Stimulation and Recording Methods

Stimulation leads (two leads; 1 cm apart) were implanted into the muscularis propria, 10 cm proximal to the pylorus midway between the greater and lesser curvature [4,20] (Figure 1B). Four stimulation protocols were assessed in each patient, as detailed in Table 1. The 'low' protocol represented the standard stimulation parameters for the Enterra device [4,20,22]. The 'medium' and 'high' protocols represented higher-energy parameters that have previously shown symptom improvements in patients with gastroparesis [23]. The 'max' protocol represented the maximum pulse-width, frequency, and voltage outputs of the device, and three combinations of on-off periods were trialled with this setting (Table 1), although each patient only received one parameter combination, to definitively define the potential for the maximal settings of this device to modulate slow waves. The choice of long stimulation intervals at the maximum settings (17s; see Table 1) was based on past studies showing successful entrainment using high-energy pulses at just above the native slow wave frequency [24,25].

Baseline HR mapping recordings were performed with stimulation off, after implantation of the stimulator leads but prior to the onset of stimulation. The four stimulation protocols were then assessed in sequential order of lowest to highest energy (i.e., Protocol 'Low' to 'Max' in Table 1). 'Washout' periods of no stimulation were additionally recorded between stimulation settings in a subset of patients (see results). After the conclusion of the experimental stimulation recordings, clinical stimulation was delivered at the 'low' setting, according to standard clinical protocol [4,20]. Stimulation parameters were subsequently increased, if required, based on patient-specific symptomatology [23].

Methods of HR Mapping

HR mapping was performed using flexible printed circuit (FPC) electrodes, comprised of 256 gold contact electrodes in a 16x16 array with an inter-electrode spacing of 4mm, using a validated extracellular technique [26,27] (Figure 1A). The FPCs were gently positioned adjacent to the site of stimulation lead implantation, either proximally over the upper to mid-corpus (e.g, Figure 4Ai), or distally over the anatomical gastric corpus-antrum border, at the level of the gastric incisura (e.g., Figure 1B), and maintained in these positions for all protocols. During normal longitudinal propagation, slow wave activity in these regions of the corpus shows a consistent stable baseline amplitude and velocity [16].

The FPCs were secured by gentle packing with warmed saline-soaked gauze and the wound edges were approximated during recordings to prevent serosal drying and

gastric cooling. The FPCs were connected by sterilized ribbon cables to an ActiveTwo system (BioSemi, Amsterdam, Netherlands) modified for passive electrode recordings, which was connected to a notebook computer running acquisition software written in LabView v8.2 (National Instruments, TX, USA). Raw data was acquired at 512 Hz.

Data analysis was performed in the Gastrointestinal Electrical Mapping Suite (GEMS) v.1.5 [28]. Recordings were down-sampled to 30 Hz, a moving median filter (20 s window) was applied for baseline removal, and a Savitzky-Golay filter (1.7 s window; polynomial order 9) was applied for high-frequency noise removal [29]. The individual data sets were then randomized for analysis, with two separate investigators assessing all recordings, blinded to the stimulation parameters. Slow wave events within these periods were automatically detected and grouped into propagating cycles using validated automated algorithms [30,31], with comprehensive manual review and correction.

Slow wave frequencies were calculated using a validated algorithm to determine temporal cycle-to-cycle intervals of successive slow wave activation times (ATs) at each electrode, which were averaged across all electrodes and also across the recorded duration for each patient [28]. Velocities were calculated using a smoothed finite difference method [32], and amplitudes were calculated by applying a peak-to-trough detection algorithm based on the 'zero-crossings' of the first and second-order signal derivatives [33]. Velocities and amplitudes were then averaged separately across regions of primarily circumferential and longitudinal propagation [34]. This is

important because velocity and amplitude vary together with a known directional conduction anisotropy, and therefore correct velocity comparisons can only be made with directionality defined [17,18,34]. The summary data and statistical comparisons are reported for typical longitudinal propagation.

Activation, velocity, and amplitude maps and dynamic animations were computed in GEMS to visualize spatial characteristics of slow wave propagation [28]. Dysrhythmias were identified by the propagation dynamics observed in the activation maps and animations, based on known patterns of normal gastric conduction [16], and a previously-developed spatiotemporal dysrhythmia classification scheme [18,19].

Statistical Methods

Patient and clinical data are presented as a median and range. HR mapping data are presented as mean ± standard deviation (SD). Differences between baseline and stimulus levels were assessed using one-way ANOVA with significance threshold defined as $P<0.05$. Comparison of TSS and gastric retention data between pre- and post-implant was performed by paired Student's t-test with significance threshold defined as $P<0.05$. For analyses of dysrhythmia rate, statistical measures of dysrhythmic duration were normalized against total recording duration to account for inherent variations in recording durations.

Results

Eight consecutive diabetic gastroparesis patients were recruited and consented, with a median age of 40.5 years (range 30 – 62), median total symptom score of 14.5 out of

20 (range 6 - 20), and median 4-hour gastric retention of 27% (range 21 – 47). Individual patient characteristics were as presented in Table 2.

HR Mapping

HR mapping recordings averaged 26 ± 5 SD minutes per patient. A total of 29 stimulation recordings and 19 control recordings (8 baseline; 11 washout periods) were collected, with an average duration of 260 ± 90 SD s per recording. Baseline recordings averaged 260 ± 120 SD s, stimulation recordings averaged 290 ± 80 SD s, and 'washout' periods between stimulation settings averaged 190 ± 70 SD s.

Figure 2 provides representative examples of slow wave activation, velocity, and amplitude field maps and electrograms during baseline and stimulation periods for one of the patients. In accordance with Figure 2, the overall cohort data also showed no difference in slow wave amplitude, velocity, or frequency between baseline and any stimulation level, or between any levels of stimulation (Figure 3; $P > 0.5$ for all). There was also no significant difference between stimulation and washout periods, or between all periods with stimulation on versus all periods with stimulation off ($P \geq 0.5$ for all). In addition, slow wave entrainment was not achieved at the longer duration on-off periods at the maximum stimulation setting (Table 1).

Dysrhythmic slow wave activity was observed in 4/8 patients, and included ectopic pacemakers, conduction blocks, retrograde propagation, and colliding wavefronts, consistent with previous observations in similar patients [17,18]. There was no difference in the occurrence of dysrhythmias with stimulation off (31% of total recorded duration was dysrhythmic) versus with stimulation on (36% of total recorded

duration was dysrhythmic), ($P > 0.5$). Figure 4 demonstrates an example dysrhythmia, a stable ectopic pacemaker arising in the mid-corpus, that occurred continuously through the baseline and stimulation periods. The velocity and amplitude field maps for the ectopic pacemaker in Figure 4 also demonstrate the rapid high-amplitude circumferential conduction known to emerge at sites of dysrhythmia [17,18,34]. This observation demonstrates the importance of defining conduction direction prior to calculating velocity and amplitude values.

Clinical Outcomes

Follow-up data were available on 6/8 patients (median time to follow-up, 5.8 months; range 4.3-6.4 months), as two patients were lost to follow-up (one passed away from diabetes-related complications unrelated to the stimulator, while a second patient did not attend local follow-up). In all patients with data, both TSS and gastric emptying improved following stimulator implantation (Table 2). Total symptom score showed a median decrease of -5.5 points (range: -8 to -4.5 points, out of 20), ($P = 0.01$), while gastric emptying showed a median 4-hour retention improvement of -8% (range: -13 to -4% retention), ($P = 0.03$).

Discussion

This study applied HR mapping to evaluate the acute spatiotemporal effects of high-frequency GES on slow wave activity in patients with diabetic gastroparesis. The results showed that a range of high-frequency GES protocols, within the dose-delivery capacity of a current commercial device, did not acutely change slow wave velocity, amplitude, or frequency, nor did they change the occurrence of slow wave dysrhythmias, which persisted at a similar rate during GES.

The *in-vivo* mapping approach applied in this study with high spatiotemporal accuracy was found to be an effective and efficient framework for investigating gastric stimulation outcomes, and can now be applied in further clinical trials to assess the efficacy of alternative stimulation protocols and devices. A significant therapeutic target would be the correction of gastric dysrhythmias, which occur in common association with nausea in multiple gastric disorders [19,35,36]. HR mapping has recently enabled accurate spatial descriptions and classifications of dysrhythmia in association with gastroparesis and chronic unexplained nausea and vomiting [17,18], and can now be used to guide a 'gastric pacing' approach [37], with parameters designed to entrain slow waves to override dysrhythmic activation, in an attempt to restore normal antegrade patterns [24]. Due to recent advances in efficient handling of massive data volumes [28], it is now possible to achieve HR mapping on-line, allowing real-time experimental trials of novel protocols targeted to dysrhythmic onset [38].

Protocol design for GES and gastric pacing is a complex task that requires optimization of a vast range of possible parameter combinations (encompassing pulse

width, amplitude, frequency, on-off timing, and electrode positions) [5,10]. In addition to HR mapping, *in-silico* modeling could also be applied in the future to help elucidate the underlying mechanisms of GES and to identify potential therapeutic protocols suitable for experimental assessment of alternative gastric pacing approaches. Recent computational simulations of GES have been beneficially coupled to experimental research [39,40], and a similar approach of coupled HR mapping and *in-silico* modelling may be of substantial value in developing gastric stimulation / pacing as a potential therapeutic option.

Although GES did not significantly affect slow wave activity in our study, the patients within this uncontrolled cohort displayed statistically significant improvements in symptoms and gastric emptying time, consistent with similar improvements shown in multiple other GES studies [7,23]. However, it should be noted that this study was not specifically powered to address these secondary outcomes. Exclusion of a placebo effect is still awaited from an adequately powered randomized clinical trial. However, clinical and animal studies have shown that high-frequency GES modulates vagal and spinal afferent pathways, affecting central nausea and vomiting centres, as well as pain thresholds, vagal efferent function and gastric sensitivity, providing alternative plausible mechanisms of action [11,12,41]. GES has also been shown to induce gastric relaxation in dogs, which has been proposed as a further potential mechanism of symptoms improvement [42].

Other data, based on sparse serosal electrode recordings, has previously suggested that GES may enhance slow wave amplitude and propagation velocity [13], but these outcomes are found to be inconsistent with our more advanced HR mapping data.

Crucially, our study highlights the importance of spatially defining the conduction direction prior to calculating extracellular slow wave amplitudes and velocities, to control for the rapid high-amplitude activity that is now known to accord with circumferential conduction, which cannot be reliably achieved through sparse-electrode methods [34]. Nevertheless, other sparse electrode studies of GES outcomes are concordant with our results by also showing minimal impact on slow waves [5,10], although such studies could not as reliably assess propagation direction, velocity and amplitude fields, or dysrhythmias.

The main limitation of this study was the acute timeframe of the mapping, performed intra-operatively after device implantation. Abell *et al.* previously suggested that the effects of GES maximize at 3 to 4 days after device implantation [43], and Williams *et al.* reported improvements in arrhythmias beyond 3 years after implantation [44]. However, Lin *et al.* previously reported entrainment of slow wave frequency in gastric pacing studies to partially occur as soon as 1 minute after stimulation, with full entrainment achieved at 5 minutes, suggesting that the average duration of mapping in this study was appropriate for identifying potential slow wave effects. Furthermore, the high-resolution mapping approach allows subtle or localized changes in slow wave parameters to be detected much earlier than with sparse electrode recordings [37] Nonetheless, slow wave mapping would ideally be conducted for longer durations, including in awake and fed patients. Mapping in conscious patients currently faces a multitude of technical barriers, but may be realised through future technical advances. Wireless transmission of gastrointestinal mapping data is one such promising recent technological advancement [45], and may be able to be coupled

with temporary endoscopic GES protocols where symptomatic improvements have been noted within 3 days [43].

Additionally, this study was limited to high-frequency GES of relatively short pulse-width (maximum 450 μs), within the parameter ranges deliverable from the commercial Enterra device. However, the robust methods of high-resolution analysis of GES in human patients that were presented in this study now provide an improved analytical platform, enabling future studies of alternative stimulation protocols, for example with wider pulse-widths and higher energies, to modulate slow wave activity [10].

A separate study from our laboratory recently reported reductions in extracellularly-recorded slow wave amplitudes in patients with gastroparesis [17]. These reduced amplitudes could result from reduced current density secondary to ICC depletion in gastroparesis [17,46], which could contribute to pathophysiology including weakened contractions. A 'field stimulation' approach to promoting more vigorous contractions could therefore offer another potential therapeutic target, and while this mechanism is excluded for the current device by our results, it could become another focus of future investigations. The spatial current distribution achieved by a stimulation device would need to be critically examined to assess whether this strategy may be feasible.

It was noted in the results that the dysrhythmia rate in our current study (50% of patients, 31-36% of recorded duration) was somewhat lower than that reported in our other recent HR mapping studies in similar populations [17,18]. This reflects the fact that only one gastric region was mapped in each patient in the current cohort, albeit

for a longer duration, whereas multiple gastric regions were targeted in the previous studies. This finding implies that in order to define dysrhythmia rates with the highest reliability in these patients, it would be beneficial to map patterns over a broader gastric area.

Conclusion

This study has demonstrated that high-frequency GES protocols achievable from a current commercial device did not acutely modulate slow wave activity or correct dysrhythmias. The methods applied here provided substantial advantages for identifying and assessing therapeutic GES parameters, and will now be applied in future studies on new parameters and devices for treating gastric disorders.

Acknowledgments

We thank the clinical research and operating room staff at the University of Mississippi Medical Center for their valued assistance.

References

1. Hasler WL. Gastroparesis: pathogenesis, diagnosis and management. *Nat Rev Gastroenterol Hepatol* 2011;**8**:438–53.

2. Wang YR, Fisher RS, Parkman HP. Gastroparesis-related hospitalizations in the United States: trends, characteristics, and outcomes, 1995-2004. *Am J Gastroenterol* 2008;**103**:313–22.

3. Tack J. The difficult patient with gastroparesis. *Best Pr Res Clin Gastroenterol* 2007;**21**:379–91.

4. Abell T, McCallum R, Hocking M *et al.* Gastric electrical stimulation for medically refractory gastroparesis. *Gastroenterology* 2003;**125**:421–8.

5. Zhang J, Chen JDZ. Systematic review: applications and future of gastric electrical stimulation. *Aliment Pharmacol Ther* 2006;**24**:991–1002.

6. Soffer E, Abell T, Lin Z *et al.* Review article: gastric electrical stimulation for gastroparesis--physiological foundations, technical aspects and clinical implications. *Aliment Pharmacol Ther* 2009;**30**:681–94.

7. O'Grady G, Egbuji JU, Du P *et al.* High-frequency gastric electrical stimulation for the treatment of gastroparesis: a meta-analysis. *World J Surg* 2009;**33**:1693–701.

8. Song G, Hou X, Yang B *et al.* Efficacy and efficiency of gastric electrical stimulation with short pulses in the treatment of vasopressin-induced emetic responses in dogs. *Neurogastroenterol Motil* 2006;**18**:385–91.

9. Song J, Zhong D-X, Qian W *et al.* Short pulse gastric electrical stimulation for cisplatin-induced emesis in dogs. *Neurogastroenterol Motil* 2011;**23**:468–74, e178.

10. Hasler WL. Methods of gastric electrical stimulation and pacing: a review of their benefits and mechanisms of action in gastroparesis and obesity. *Neurogastroenterol Motil* 2009;**21**:229–43.

11. McCallum RW, Dusing RW, Sarosiek I *et al.* Mechanisms of symptomatic improvement after gastric electrical stimulation in gastroparetic patients. *Neurogastroenterol Motil* 2010;**22**:161–7, e50–1.

12. Gourcerol G, Ouelaa W, Huet E *et al.* Gastric electrical stimulation increases the discomfort threshold to gastric distension. *Eur J Gastroenterol Hepatol* 2013;**25**:213–7.

13. Lin Z, Forster J, Sarosiek I *et al.* Effect of high-frequency gastric electrical stimulation on gastric myoelectric activity in gastroparetic patients. *Neurogastroenterol Motil* 2004;**16**:205–12.

14. Cheng LK, Du P, O'Grady G. Mapping and modeling gastrointestinal bioelectricity: from engineering bench to bedside. *Physiol* 2013;**28**:310–7.

15. Lammers WJEP, Stephen B, Arafat K *et al.* High resolution electrical mapping in the gastrointestinal system: initial results. *Neurogastroenterol Motil* 1996;**8**:207–16.

16. O'Grady G, Du P, Cheng LK *et al.* Origin and propagation of human gastric slow-wave activity defined by high-resolution mapping. *Am J Physiol Gastrointest Liver Physiol* 2010;**299**:G585–92.

17. O'Grady G, Angeli TR, Du P *et al.* Abnormal initiation and conduction of slow-wave activity in gastroparesis, defined by high-resolution electrical mapping. *Gastroenterology* 2012;**143**:589–98.e1–3.

18. Angeli TR, Cheng LK, Du P *et al.* Loss of interstitial cells of Cajal and patterns of gastric dysrhythmia in patients with chronic unexplained nausea and vomiting. *Gastroenterology* 2015;**149**:56–66.e5.

19. O'Grady G, Wang T, Du P *et al.* Recent progress in gastric arrhythmia: pathophysiology, clinical significance and future horizons. *Clin Exp Pharmacol Physiol* 2014;**41**:854–62.

20. McCallum RW, Snape W, Brody F *et al.* Gastric electrical stimulation with Enterra therapy improves symptoms from diabetic gastroparesis in a prospective study. *Clin Gastroenterol Hepatol* 2010;**8**:947–54.e1.

21. Abell TL, Camilleri M, Donohoe K *et al.* Consensus recommendations for gastric emptying scintigraphy: a joint report of the American Neurogastroenterology and Motility Society and the Society of Nuclear Medicine. *Am J Gastroenterol* 2008;**103**:753–63.

22. Familoni BO, Abell TL, Nemoto D *et al.* Efficacy of electrical stimulation at frequencies higher than basal rate in canine stomach. *Dig Dis Sci* 1997;**42**:892–7.

23. Abidi N, Starkebaum WL, Abell TL. An energy algorithm improves symptoms in some patients with gastroparesis and treated with gastric electrical stimulation. *Neurogastroenterol Motil* 2006;**18**:334–8.

24. McCallum RW, Chen JD, Lin Z *et al.* Gastric pacing improves emptying and symptoms in patients with gastroparesis. *Gastroenterology* 1998;**114**:456–61.

25. Lin ZY, McCallum RW, Schirmer BD *et al.* Effects of pacing parameters on entrainment of gastric slow waves in patients with gastroparesis. *Am J Physiol* 1998;**274**:186–91.

26. Du P, O'Grady G, Egbuji JU *et al.* High-resolution mapping of in vivo gastrointestinal slow wave activity using flexible printed circuit board electrodes: methodology and validation. *Ann Biomed Eng* 2009;**37**:839–46.

27. Angeli TR, Du P, Paskaranandavadivel N *et al.* The bioelectrical basis and validity of gastrointestinal extracellular slow wave recordings. *J Physiol* 2013;**591**:4567–79.

28. Yassi R, O'Grady G, Paskaranandavadivel N *et al.* The gastrointestinal electrical mapping suite (GEMS): software for analyzing and visualizing high-resolution (multi-electrode) recordings in spatiotemporal detail. *BMC Gastroenterol* 2012;**12**:60.

29. Paskaranandavadivel N, O'Grady G, Du P *et al.* Comparison of filtering methods for extracellular gastric slow wave recordings. *Neurogastroenterol Motil* 2013;**25**:79–83.

30. Erickson JC, O'Grady G, Du P *et al.* Falling-edge, variable threshold (FEVT) method for the automated detection of gastric slow wave events in high-resolution serosal electrode recordings. *Ann Biomed Eng* 2010;**38**:1511–29.

31. Erickson JC, O'Grady G, Du P *et al.* Automated gastric slow wave cycle partitioning and visualization for high-resolution activation time maps. *Ann Biomed*

Eng 2011;**39**:469–83.

32. Paskaranandavadivel N, O'Grady G, Du P *et al.* An improved method for the estimation and visualization of velocity fields from gastric high-resolution electrical mapping. *IEEE Trans Biomed Eng* 2012;**59**:882–9.

33. Paskaranandavadivel N, Cheng LK, Du P *et al.* Improved signal processing techniques for the analysis of high resolution serosal slow wave activity in the stomach. *Conf Proc IEEE Eng Med Biol Soc* 2011;**1**:1737–40.

34. O'Grady G, Du P, Paskaranandavadivel N *et al.* Rapid high-amplitude circumferential slow wave propagation during normal gastric pacemaking and dysrhythmias. *Neurogastroenterol Motil* 2012;**24**:e299–312.

35. Koch KL. Gastric dysrhythmias: a potential objective measure of nausea. *Exp Brain Res* 2014;**232**:2553–61.

36. O'Grady G, Abell TL. Gastric arrhythmias in gastroparesis: low- and high-resolution mapping of gastric electrical activity. *Gastroenterol Clin N Am* 2015;**44**:169–84.

37. O'Grady G, Du P, Lammers WJEP *et al.* High-resolution entrainment mapping of gastric pacing: a new analytical tool. *Am J Physiol Gastrointest Liver Physiol* 2010;**298**:G314–21.

38. Bull S, O'Grady G, Du P *et al.* A system and method for online high-resolution mapping of gastric slow wave activity. *IEEE Trans Biomed Eng* 2014;**61**:2679–87.

39. Du P, Li S, O'Grady G *et al.* Effects of electrical stimulation on isolated rodent gastric smooth muscle cells evaluated via a joint computational simulation and experimental approach. *Am J Physiol Gastrointest Liver Physiol* 2009;**297**:G672–80.

40. Du P, O'Grady G, Windsor JA *et al.* A tissue framework for simulating the effects of gastric electrical stimulation and in vivo validation. *IEEE Trans Biomed Eng* 2009;**56**:2755–61.

41. Ouelaa W, Ghouzali I, Langlois L *et al.* Gastric electrical stimulation decreases gastric distension-induced central nociception response through direct action on primary afferents. *PLoS One* 2012;**7**:e47849.

42. Xing JH, Brody F, Brodsky J *et al.* Gastric electrical stimulation at proximal stomach induces gastric relaxation in dogs. *Neurogastroenterol Motil* 2003;**15**:15–23.

43. Abell TL, Johnson WD, Kedar A *et al.* A double-masked, randomized, placebo-controlled trial of temporary endoscopic mucosal gastric electrical stimulation for gastroparesis. *Gastrointest Endosc* 2011;**74**:496–503.e3.

44. Williams PA, Nikitina Y, Kedar A *et al.* Long-term effects of gastric stimulation on gastric electrical physiology. *J Gastrointest Surg* 2013;**17**:50–6.

45. Paskaranandavadivel N, Wang R, Sathar S *et al.* Multi-channel wireless mapping of gastrointestinal serosal slow wave propagation. *Neurogastroenterol Motil* 2015;**27**:580–5.

46. Grover M, Farrugia G, Lurken MS *et al.* Cellular changes in diabetic and idiopathic gastroparesis. *Gastroenterology* 2011;**140**:1575–85.e8.

Tables

Table 1: Stimulation Settings

Protocol	Amplitude (mA)	Pulse-Width (μs)	Frequency (Hz)	On Period (s)	Off Period (s)
Low[†]	5	330	14	0.1	5
Medium	10	330	28	1	4
High[‡]	19.2 ± 0.9	450	55	4	1
Max[‡,§]	19.2 ± 0.9	450	130	4	1
				1	17
				0.5	17

[†]The 'Low' protocol is the standard Enterra protocol [4,20]; [‡]for the 'High' and 'Max' settings, voltage was delivered at the maximum output of the device such that the delivered amplitude varied based on the impedance at the stimulator leads, and is reported here as a cohort average ± SD; [§]multiple on-off periods were also investigated for the 'Max' setting, as noted, although each patient only receive one parameter combination.

Table 2: Patient baseline characteristics and post-operative stimulation outcomes

Patient ID	Age (years)	Sex	BMI	Pre-Implant TSS (out of 20)†	Post-Impant TSS (out of 20)†	Pre-Op 4-hr Gastric Retention (%)	Post-Op 4-hr Gastric Retention (%)
1	30	M	27.8	13	No Data	26.9	No Data
2	39	M	27.3	No Data	7.5	41	No Data
3	32	M	21.2	14.5	No Data	21.5	No Data
4	57	M	46.2	6	0	21	17
5	30	M	20.5	17.5	13	34	23
6	50	F	31.6	18	13	27	No Data
7	42	M	25.3	14	8.5	47	42
8	62	M	32.5	20	12	25	12
Median:	**40.5**	**-**	**27.6**	**14.5**	**10.3**	**27**	**20**

†TSS ('total symptom score') is a combined metric for the severity of nausea, vomiting, early-satiety, pain, and bloating [17].

Figure Legends

Figure 1

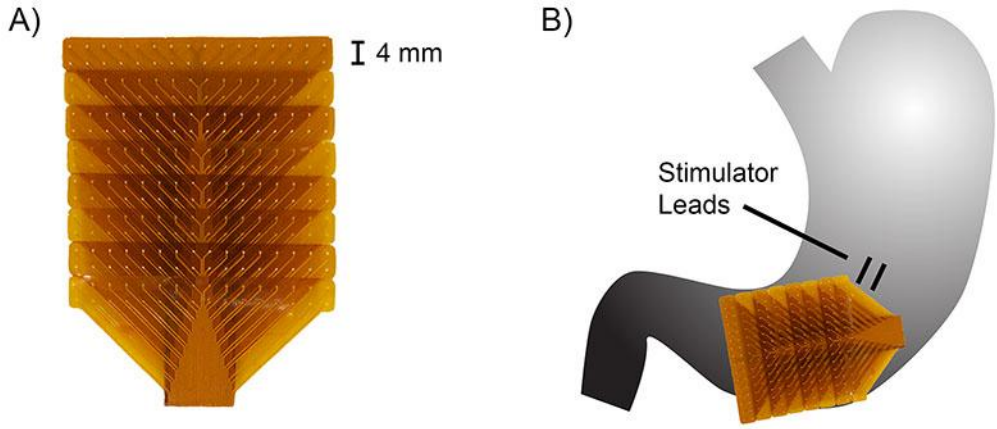

Figure 1: Illustration of methods. **A)** FPC electrode array. **B)** Typical positioning of the stimulator leads and distal positioning of the FPC electrode array on the stomach.

Figure 2

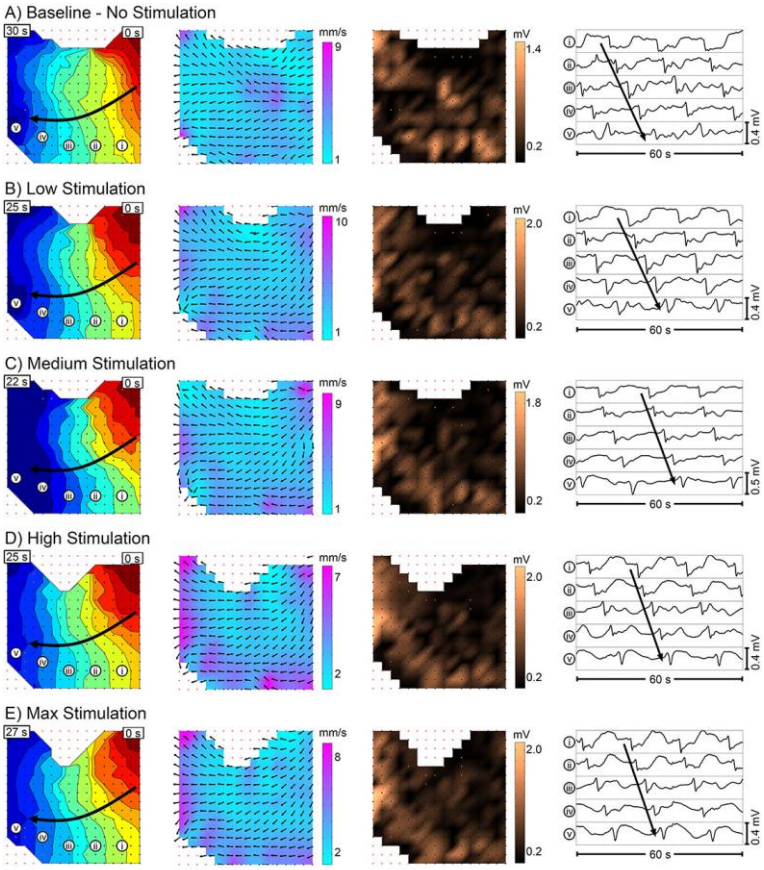

Figure 2: Example slow wave maps showing (from left to right) activation, velocity, and amplitude, during periods of **A)** baseline, **B)** low stimulation, **C)** medium stimulation, **D)** high stimulation, and **E)** max stimulation. Activation maps show the propagation pattern of a single wavefront, with each color band representing the area of propagation per 2 s, from red (early) to blue (late). Each dot represents an electrode, and red outlined dots signify that data was interpolated at that electrode. Velocity maps show the direction (arrow) and speed (color gradient) of propagation of the wavefront at each electrode. Amplitude maps show the slow wave amplitude at each electrode as a color gradient across the array. Example electrograms are shown in the right-most column, corresponding to the electrode positions labelled in the activation map (left-most column). The FPC electrode array was positioned in the distal antrum for these recordings, as shown in Figure 1B.

Figure 3

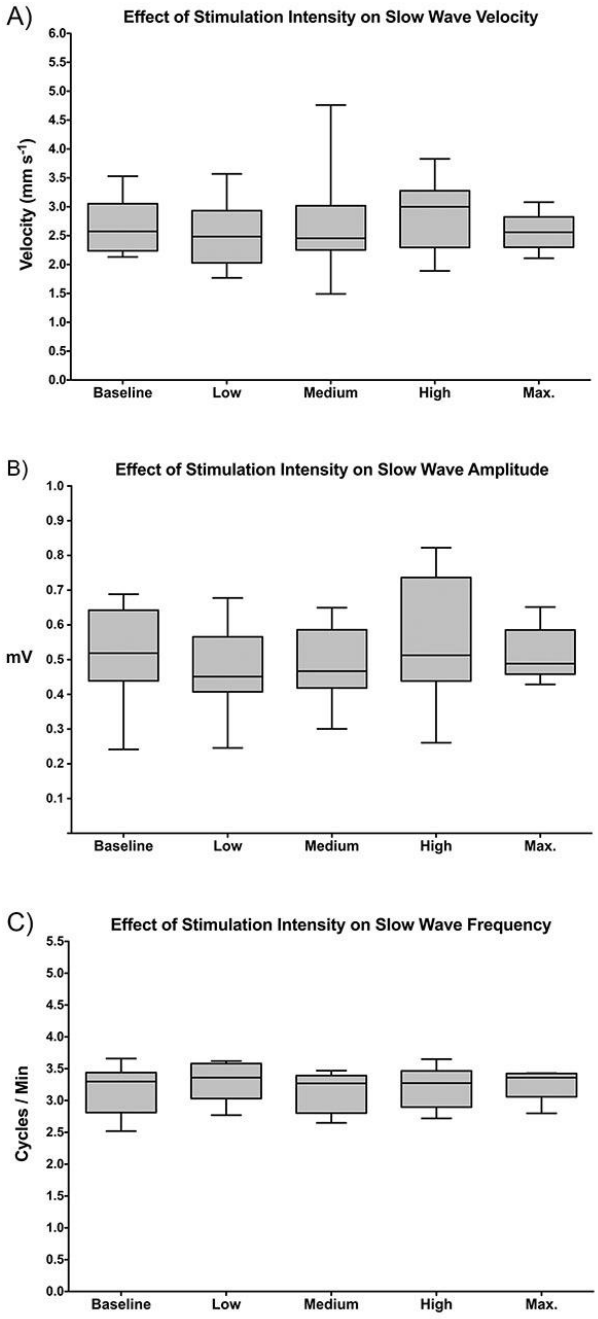

Figure 3: Average slow wave characteristics compared at baseline and each level of stimulation, including: **A)** longitudinal velocity, **B)** amplitude, and **C)** frequency. Washout periods with stimulation off were also performed between stimulation levels (refer to text).

Figure 4

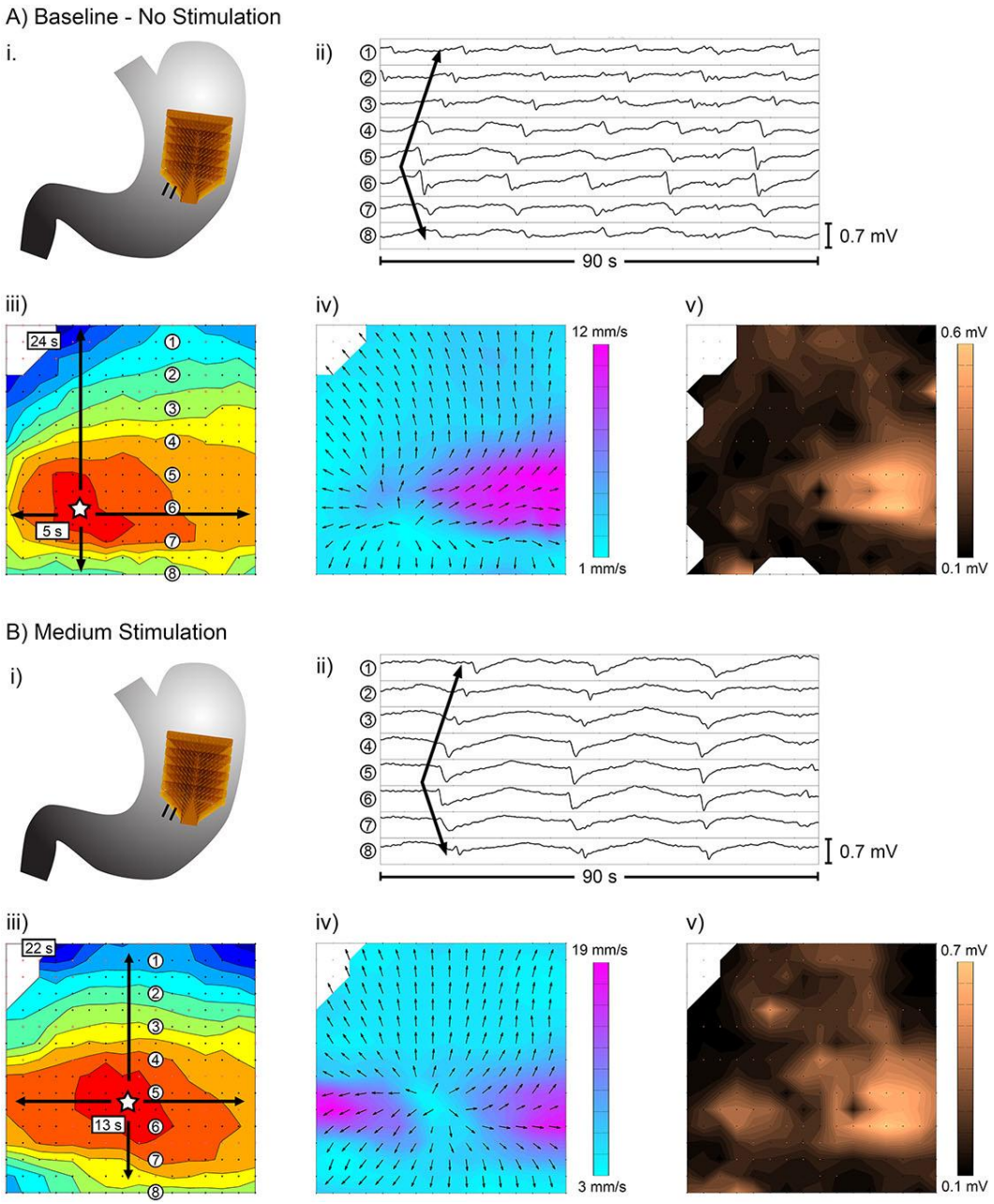

Figure 4: Example dysrhythmic slow wave propagation in a **A)** baseline recording (stimulation off) versus **B)** recording during stimulation (medium protocol). **i)** position of the electrode array; **ii)** example electrograms from electrodes labelled in panel *iii*; **iii-v)** activation, velocity, and amplitude maps, respectively, as described in Figure 2.